MODELING OF GLOBAL BUCKLING OF LONGITUDINAL REINFORCEMENT

Leonardo M. Massone & Eduardo E. López
University of Chile, Chile

SUMMARY:
The longitudinal reinforcement within reinforced concrete elements could be subjected to large compressive strains under severe earthquakes, resulting in buckling. Observations have shown that this phenomenon may result in a buckling length larger than the spacing between transverse reinforcement, deforming the stirrups (global buckling of reinforcement). The behavior of the longitudinal reinforcement in monotonic compression considering the case of global buckling is studied in this work, based on a fiber concentrated plasticity model that considers four (4) plastic hinges, introducing the effect of transverse reinforcing and expansion of the core concrete in the analysis. The proposed model is validated by comparison of the model buckling mode with experimental results in the literature. The average error in the prediction of buckling mode is -0.59 (about half the space between stirrups), which is a reasonably good value considering that the database of tests used covers failure modes from 1 to 7 (stirrup spacing).

Keywords: buckling; reinforcement; reinforced concrete; columns; model

1. INTRODUCTION

In a seismic context, the actions imposed by a major event can bring an element to its limit strength and deformation, yielding different types of failure. Elements designed to withstand significant forces and deformations in compression, such as columns or walls, need to be study accounting for potential loss of resistance generated by the buckling of longitudinal reinforcement. It has been observed that the concrete cover, since it is not confined, spalls at longitudinal strains between 0003 and 0004 (Papia et al., 1988), therefore, the effective lateral restraint and restriction to buckling of longitudinal reinforcement is given by the stirrups.

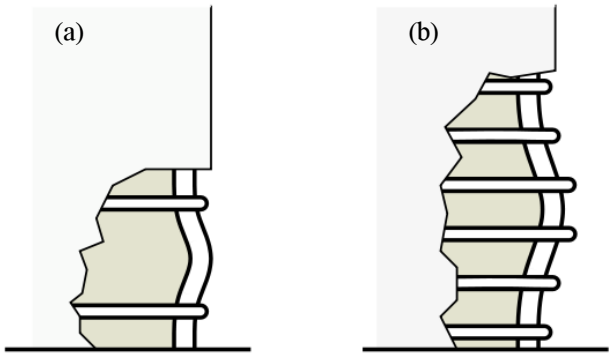

Figure1. (a) Local bar buckling, (b) Global bar buckling

Usually, buckling of longitudinal reinforcement is considered located in a length determined by the distance between stirrups, which is called local buckling of the reinforcement (Fig. 1a). However, experimental observations have shown that in elements with a good distribution of stirrups, the buckling length may be longer, stretching those stirrups that are within the buckling length and

prevailing over the local buckling. This is called global buckling of the reinforcement (Fig. 1b). Thus, the buckling length is not completely determined by the spacing of stirrups, but also by the flexibility of the reinforcement (longitudinal and transversal). In order to study this phenomenon it is necessary to appropriately reproduce the behavior of the elements involved in rebar buckling.

The objective of this work is to use an existing model, Massone & Moroder (2009), which has shown good performance in representing the local buckling of reinforcing and extending their application to global buckling in monotonic analysis.

2. CONCENTRATED PLASTICITY MODEL – LOCAL BUCKLING

The model described by Massone and Moroder (2009) is used to study the buckling response of bare longitudinal reinforcement, which captures the behavior of reinforcement in monotonic compression without constrains in its length, and has been slightly modified by Lacaze (2009). The original model considers a bar with fixed ends free to move vertically in its upper end, with an initial imperfection given by a lateral displacement in the middle of its length. The deformations are concentrated in four plastic hinges located symmetrically at positions of maximum moment for a point load or imperfection e applied at the bar mid-length. Additional lateral deformation w is associated to a vertical displacement v of the free end due to an applied load p. The plastic hinge length is set as the bar diameter, $l_p = d$, with a constant curvature distribution along it, such that the hinge rotation, θ, is related to the curvature ϕ as $\theta = \phi \cdot l_p$. The imperfection e can be introduced as an initial rotation.

At the beginning of the axial loading, the load p and the moment m at the hinge are zero. A vertical displacement v of the upper end has an associated additional rotation of the hinge θ_p and a lateral displacement of the central zone of the bar w. Lacaze (2009) introduces a change in the original model in order to represent cyclic behavior and properly represent the response in tension without hinge formation. For this purpose, rotations (curvatures) are concentrated at the plastic hinge, but axial deformations are distributed along the bar.

The internal forces in the hinge are determined by the axial strain, ε, and the curvature, ϕ. The cross-section is discretized into a finite number of axially deformable fibers (20), where each fiber has a strain $\varepsilon_i = \varepsilon + \phi x_i$, assuming the Bernoulli hypothesis, where x_i is the location of the fiber. By means of the constitutive material law, the steel stress is obtained for each fiber (σ_i), resulting, by equilibrium, in a resultant axial force and moment at the hinge.

The numerical nonlinear problem is reduced to a 1 DOF, where given an axial deformation, $\bar{\varepsilon}$, the formulation iterates over the value for the plastic curvature, ϕ_p, until equilibrium $m = p(e+w)/2$ is achieved (within a tolerance). The currently implemented model considers that the initial imperfection is present in the bar without residual stresses, i.e., the bar was not deformed but naturally has an imperfection. For straight bars, to avoid obtaining the solution without buckling effect (trivial solution), the model assumes an imperfection $e = 0.01d$, where d is the diameter of the longitudinal reinforcement.

Reinforcing steel in tension is modeled as suggested by Mander et al. (1984). The model considers an elasto-plastic behavior with initial stiffness E_s, and a yield stress and strain point given by (σ_y, ε_y). Strain hardening starts from an strain value of ε_{sh} governed by the relationship $\sigma_s = \sigma_m + (\sigma_y - \sigma_m)\left|\frac{\varepsilon_s - \varepsilon_m}{\varepsilon_{sh} - \varepsilon_m}\right|^p$, where $p = E_{sh}\left(\frac{\varepsilon_m - \varepsilon_{sh}}{\sigma_m - \sigma_y}\right)$ and ends at the point (ε_m,σ_m) where the peak stress is reached. A linear degradation is defined from the peak stress point to the fracture point (ε_u, σ_u).

Commonly, steel compression behavior is represented by the same curve as for the steel in tension. However, the use of engineering coordinates (referred to initial length and cross-section)

gives no reliable values given the reinforcement cross-section and length variation. The use of true coordinates allows considering the fact that the area changes as the load is applied. The response in compression taken as identical to tension in true coordinates provides a good correlation until reaching the buckling load. Thus, deformations in tension and compression may be written with respect to the values in tension, such that $\sigma_{s,c} = -\sigma_{s,t}(1+\varepsilon_{s,t})^2$ and $\varepsilon_{s,c} = -\dfrac{\varepsilon_{s,t}}{1+\varepsilon_{s,t}}$, where $\sigma_{s,c}$ and $\varepsilon_{s,c}$ refer to the values of compression stress and strain in engineering coordinates (negative) and $\sigma_{s,t}$ and $\varepsilon_{s,t}$ are those corresponding to tensile stress and strain (positive), as indicated by Dodd and Restrepo-Posada (1995).

The steel cyclic model is based on a simple phenomenological formulation that requires unloading and reloading rules. In principle, the curves for the tensile and compressive monotonic steel are maintained, but outside the linear range the unloading point continues towards a point (end) with the same strain as in the previous reloading point, according to curve A (Fig. 2), which represents the Bauschinger effect. Curve A can be used as a transition point between unloading/reloading points, which has the form $\sigma_s = \sigma_0 + E_0(\varepsilon_s - \varepsilon_0)\left(Q + (1-Q)/\left(1+\left(E_o\left(\dfrac{\varepsilon_s-\varepsilon_0}{\sigma_f-\sigma_0}\right)\right)^R\right)^{1/R}\right)$, where R is the parameter representing the Bauschinger effect (the smaller the value of R, the smoother the transition), E_0 is the initial elastic reloading/unloading module, ε_0 and σ_0 are strain and stress at the beginning of curve A, and ε_f and σ_f are the strain and stress at the end of curve A. The parameter Q is defined as $Q = (E_{sec}/E_0 - a)/(1-a)$, with $E_{sec} = (\sigma_f - \sigma_0)/(\varepsilon_f - \varepsilon_0)$ and $a = \left(1+(E_0/E_{sec})^R\right)^{-1/R}$. The values of E_0 and R used by Massone and Moroder (2009), originally obtained by Mander et al. (1984), were modified by Lacaze (2009) to improve cyclic response of the reinforcement. Thus, $E_0 = E_s(1-\Delta\varepsilon)$ and for the unloading stage $R = 14\left(\varepsilon_y\right)^{1/3}(1-14\Delta\varepsilon)$ is used, whereas for the reloading stage $R = 20\left(\varepsilon_y\right)^{1/3}(1-18\Delta\varepsilon)$ is considered, where $\Delta\varepsilon = |\varepsilon_f - \varepsilon_0|/2$.

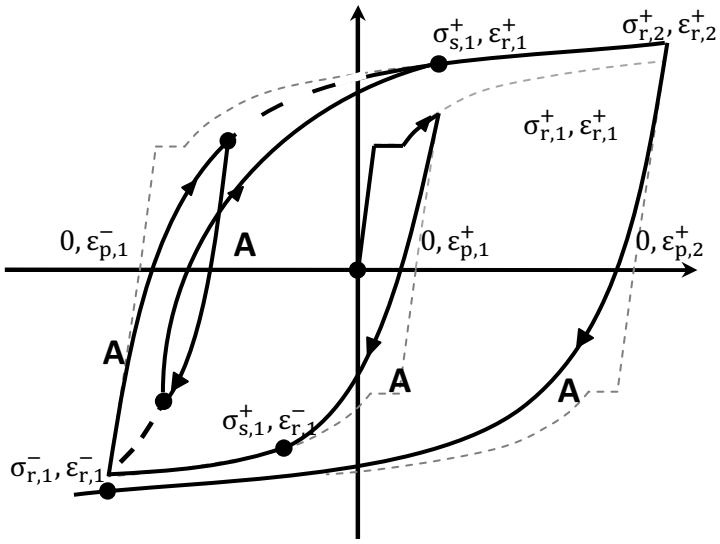

Figure 2. Cyclic steel model (Massone and Moroder, 2009 modified by Lacaze, 2009)

The implementation for the first cycle involves knowing the end point of curve A, which is obtained originally by first shifting the steel envelope stress-strain curve to a point where elastic unloading results in zero stress, and then estimating the stress in the shifted curve at zero strain. However, Lacaze (2009) compared results obtained with this modeling approach and test results for the first cycle, and improved it by taking the final point as the yield strain point. For subsequent cycles

the start and end points correspond to points (strains) at the previous unloading and reloading points. After reaching the end of curve A, it returns to the shifted monotonic envelope. For internal cycles the end point corresponds to the start of the outer loop, rather than the inside loop (Fig. 2).

3. CONCENTRATED PLASTICITY MODEL – GLOBAL BUCKLING

In order to introduce the global buckling, the main model attributes for the concentrated plasticity model by Massone and Moroder (2009), modified by Lacaze (2009) are considered. Global buckling incorporates the interaction with stirrups along the buckled shape of the longitudinal reinforcement, as well as the impact of concrete expansion. Thus, overall response of longitudinal reinforcement in columns or wall boundary elements can be studied with the formulation.

The buckling length, L, is determined by the mode of buckling considered in the analysis, so that the mode has an associated $mode\ i$ along $L_{mode\ i} = i \cdot S$, with S the spacing between stirrups, so that local buckling of reinforcement is represented by $mode\ 1$, and, in general, the total number of stirrups considered for the analysis is given by $N = i + 1$. For superior modes, the model requires that at early stages of compressive strains concrete cover spalls, so that the constraining effect from the stirrups prevent or delay buckling.

Previous researches have considered (e.g. Papia et al., 1988; Pantazopoulou, 1998) that the lateral expansion of concrete is enough to cause the stirrups large strains such that they are in the hardening region of the steel stress-strain response once buckling of longitudinal reinforcement occurs. On the other hand, Dhakal and Maekawa (2002) indicated that the expansion by itself is not enough to take the stirrup beyond the elastic range; implementing a model approach that considers that the expansion of concrete consumes all the elastic deformation of the steel within the buckled zone, but remains in the elastic zone where the concrete expansion is more relevant than buckling. Thus, the concrete contribution should not be neglected. In fact, ignoring the concrete expansion effect practically leads to only local buckling, that is, between two consecutive stirrups, given their high stiffness and strength. Thus, for stirrups within the buckling length of the longitudinal reinforcement, two sources of deformation are considered: first, the lateral expansion undergone by the confined concrete and second, the additional tensile strain provided by lateral displacement of the longitudinal bar once buckling starts.

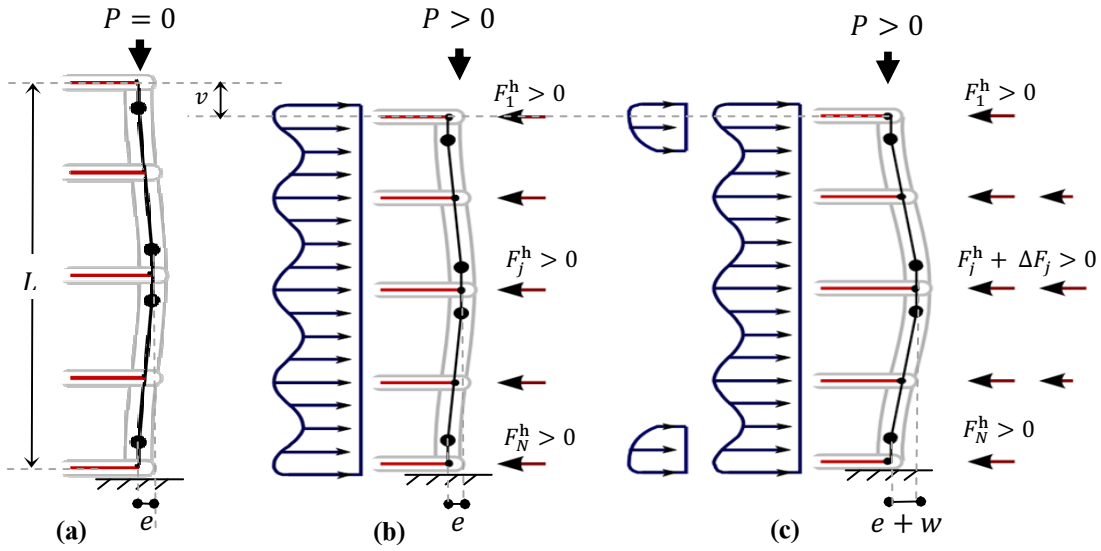

Figure 3. Global buckling model – (a) initial condition (imperfection), (b) concrete core expansion (no buckling), (c) concrete expansion and bar buckling

The bar that is susceptible of buckling is initially in contact with the concrete core, but once buckling starts lateral confinement is reduced facilitating the expansion of the concrete inside the buckled length of the bar, so that, no contact is lost between reinforcement and concrete. Thus, the forces are transmitted from the stirrups to the concrete core, as well as to internal stresses of the longitudinal bar. In order to introduce the force in the stirrups, initially, an intermediate stage (fictitious) would be considered, where for an axial imposed strain, $\bar{\varepsilon}$, associated to a vertical displacement v, the bar does not buckle, Fig. 3(b), and strains in the stirrups are only due to the lateral expansion of the concrete core, ε_{ct}, considered identical for all stirrups. Under these conditions, the stirrups forces only due to the concrete expansion, F_j^h, are transmitted completely to the concrete core.

When considering the longitudinal reinforcement buckling, an additional strain is introduced into each stirrup, ε_{wj}, which is associated to a force increment, ΔF_j, as shown in Fig. 3(c). These additional forces are balanced by internal moments at the hinges, regardless of an increase in the concrete core within the buckled bar length (forces in concrete are only added at the ends of the buckled length). The internal moment of a hinge, M, is the same for all hinges because the rotation in them is equal, balancing the additional forces in the stirrups, ΔF_j, and the moment generated by the eccentricity of the axial force, $P \cdot (e + w)$. Then, the analysis is reduced to capture the effect of incremental forces on the bar, and given the symmetry only half of the total bar length is considered, as shown in Fig 4. Thus, the problem considers the stirrups 1 to N', where N' depends on whether N (number of stirrups within the buckled bar length) is even (N'=N/2) or odd (N'=(N+1)/2), where in the case of odd value of N, half of the force $F_{N'}^h$ should be considered. It is considered that the forces ΔF_j act perpendicular to the main direction of reinforcement, i.e., the stirrups only work in tension, neglecting other actions. Then the equilibrium equation for the hinges in the middle of the bar is given by Equation (1), where x_t is the eccentricity of the external axial force P, determined by $x_t = e + w$ and x_j is the vertical distance of the force ΔF_j relative to the extreme hinge, which in the case of Fig. 4 corresponds to the upper hinge.

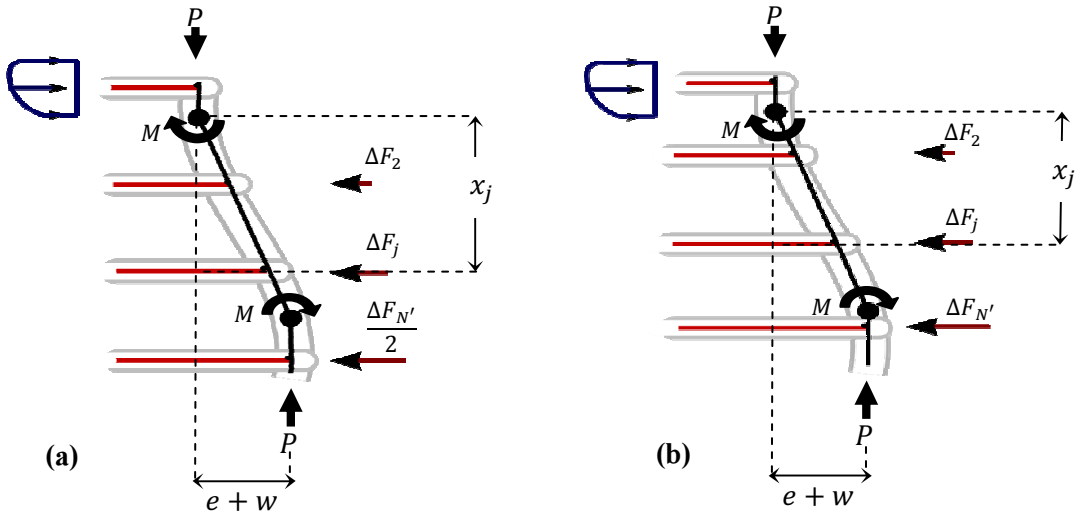

Figure 4. Equilibrium buckled bar (half length) – (a) N even, (b) N odd

$$P \cdot x_t + \sum_{j=2}^{N'} \Delta F_j \cdot x_j - 2 \cdot M = 0 \qquad (1)$$

Since when the upper end moves the longitudinal bar inclines, the distance x_j varies as displacement of the upper end, v, increases. It is assumed that the stirrup does not slide with respect to the longitudinal bar and therefore the force exerted by each stirrup is firmly joined to a fixed point of the model.

3.1. Forces in stirrups

As stated earlier, in order to correctly characterize the response of stirrups the concrete core expansion as well as the additional deformation that comes from the buckled bar should be considered. The total force action on each stirrup, F_j, is determined by the total strain, which considers both the deformation due to the concrete lateral expansion ε_{ct} and the lateral deformation that imposes the buckled bar, ε_{wj}. Thus, the force is estimated as $F_j = A_t\sigma_{st}(\varepsilon = \varepsilon_{wj} + \varepsilon_{ct})$, where A_t is the cross sectional area of the stirrup, and $\sigma_{st}(\varepsilon)$ is the steel stress for a strain ε. Two steel models are considered to characterize the steel response of stirrups to better capture the available experimental data (Menegotto and Pinto, 1973; Mander et al., 1984). In both cases, after reaching the maximum stress, the capacity remains constant.

The force ΔF_j corresponds to the additional force above the one introduced by concrete expansion, F_j^h, which is described as $\Delta F_j = F_j - F_j^h$, where $F_j^h = A_t f_{st}(\varepsilon_{ct})$. The strain ε_{ct} is dependent of the average axial strain $\bar{\varepsilon}$ within the buckling length. These assumptions are considered, given the little information available to determine ΔF_j, that is, the additional forces in the stirrups caused by buckling of the longitudinal reinforcement.

3.1.1. Stirrup strain due to longitudinal bar buckling, ε_{jw}

Strains or stresses in stirrups are considered, in part, as a resultant from the displacements induced by bar buckling, acting in each contact point in the opposite direction to buckling (inward), which as a simple formulation can represent common configurations of stirrups (mainly in rectangular columns) and one of the most probable cases of buckling due to its lower stiffness (Fig. 5a), as it is pointed out by Papia et al. (1988). Due to this, corner bars are considered to buckle in the main directions. Thus, the stirrup strain is given by $\varepsilon_{jw} = y_j / l_t'$, where l_t' is the effective length of the stirrup, which can be regarded as the total length (l_t) or half the length ($l_t/2$) depending if the column is in bending or concentric compression , respectively. In case of concentric compression (Fig. 5a), it is supposed that there is simultaneity and symmetry of buckling (two opposite sides of the column), such that each longitudinal reinforcement bar acts on a length equal to half the total length of the stirrup. In case of bending, the bars are prone to buck in the region of highest compression of the element section (one side only of the column), acting over the total length of the stirrup, as the bars of the other end is being loaded in tension or with a lower level of compression, indicating that it will not suffer buckling or will occur at a later stage.

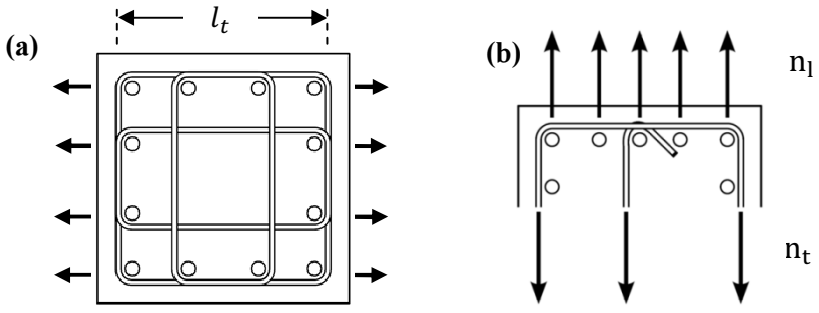

Figure 5. (a) direction analysis for buckling, (b) group bar buckling

3.1.2. Concrete core expansion, ε_{ct}

Deformation due to lateral expansion of the concrete (ε_{ct}) is usually considered uniform along the height of the element, which applies that is equal in all stirrups. This strain can be determined with the expression $\varepsilon_2 = -\nu\varepsilon_c + (1-2\nu)\frac{k_e\rho_s f_{yt}}{E_c} - \varepsilon_{cc}\frac{(1-2\nu)}{2}\left(\frac{\varepsilon_c - 0.00015/\nu}{\varepsilon_{cc} - 0.00015/\nu}\right)^2$ by Pantapozoulou

(1998) for any axial strain ε_c, where $\varepsilon_{cc} = \varepsilon_0 \left(1 + \frac{24.6 k_e \rho_s \sigma_{yt}}{f'_c} \right)$ is the confined concrete compressive strain at the maximum stress, ρ_s is the amount of volumetric transverse reinforcement, σ_{yt} is the yield stress, E_c is the concrete elastic modulus, f'_c is the unconfined compressive strength of concrete and ε_0 the correspondent strain, ν corresponds to the initial Poisson's ratio, which is taken as 0.2. The effectiveness factor of confinement k_e is determined as in Mander et al. (1988), as indicated by Pantazopoulou (1998). This equation is based on the behavior of concrete with a constant lateral pressure, yielding to uniform strain distribution without showing the reduction of strain expected at the stirrup location, since on these places there is a higher local confinement. Even this small shortcoming this expansion model is chosen, since it is one of the few reported in the literature and requires parameters that are normally determined in common tests.

In order to represent the impact of stirrups in the local expansion at their location, a calibration factor k_v is introduced by weighting the volumetric expansion component of the original expression. Besides, for simplicity, the term associated directly to confinement is removed given that confinement is already taking into account. Thus, the expression reduces to,

$$\varepsilon_{ct} = -\nu\varepsilon_c - k_v \varepsilon_{cc} \frac{(1-2\nu)}{2} \left(\frac{\varepsilon_c - 0.00015/\nu}{\varepsilon_{cc} - 0.00015/\nu} \right)^2 \quad (2)$$

Factor k_v that multiplies the volumetric expansion component of Equation (2) is calibrated according to experimental measurements to adjust the measured strains in the stirrups resulting from the expansion of the concrete. For this purpose, the tests carried out by Sheikh and Uzumeri (1980) are considered. Least squares method is used to calibrate k_v to the data obtained experimentally, yielding an average value of $k_v = 0.33$.

3.2. Methodology – buckling of group bars

The analysis of elements such as walls or columns with longitudinal reinforcement prone to buckle, requires defining the number bars that might buckle on one side of the section (n_l), and the number of legs of stirrups providing support against buckling in that direction (n_t), as shown in Fig. 5b. The original equilibrium equation (1) for bare bar under buckling is modified to account for all reinforcement involved in group bar global buckling (longitudinal bars and stirrups) by weighting the corresponding forces (or moment) by n_l and n_t, depending on whether they correspond to longitudinal or transverse reinforcement, respectively, similarly as used by Dhakal and Maekawa (2002), yielding:

$$n_l \cdot P \cdot x_t + n_t \cdot \sum_{j=2}^{N'} \Delta F_j \cdot x_j - n_l \cdot 2 \cdot M = 0 \quad (3)$$

This methodology attempts to capture an average behavior of all bars, rather than an individual behavior, so that it makes no distinction between bars directly constrained by a stirrup bar or an intermediate bar.

3.2.1. Critical buckling length selection

The analysis considers a known buckling length, *L*, however, in reality this length depends on the characteristics of the longitudinal reinforcement and the restriction presented by the stirrups to buckling. Thus, the buckling length can range from stirrups spacing, *S* (local buckling) to a length of several spacings. Local buckling occurs when there is a very high axial stiffness of the stirrups compared with the flexural stiffness of the longitudinal reinforcement, as is the case of very thick stirrups or very slender longitudinal reinforcement because of a large separation of stirrups or a small longitudinal reinforcement diameter.

As a selection criterion it is considered that the buckling mode that yields the lower peak capacity is the probably mode, which corresponds to a simple condition consistent with the criterion used by other researchers to estimate the critical buckling load (e.g., Papia et al., 1988, Pantazopoulou, 1998, and Dhakal and Maekawa, 2002). Due to the shape of the overall stress-strain curves there are two types of behavior: the most common is that the maximum is at a value higher than the yield stress (e.g., Fig. 6 – L/s= 3 selected) and another where the differentiation of the curves occurs soon after a drop past yielding, in which case the second peak is considered for the analysis. This is because the major transverse displacement caused by buckling occurs after exceeding the first maximum. Although, this methodology requires this additional effort, its rewards lies in the fact that the stress-strain can also be obtained.

As in this methodology it is required to analyze the behavior of the bar from the local buckling mode and so on, in some configurations, this involves analyzing the buckling of a bar with slenderness (L/d) less than 4 due to the relatively short distance between stirrups. The original model considers that the plastic hinge length is the diameter of the reinforcement (d). Thus, to avoid the overlap of the 4 plastic hinges, their length is limited to L/4.

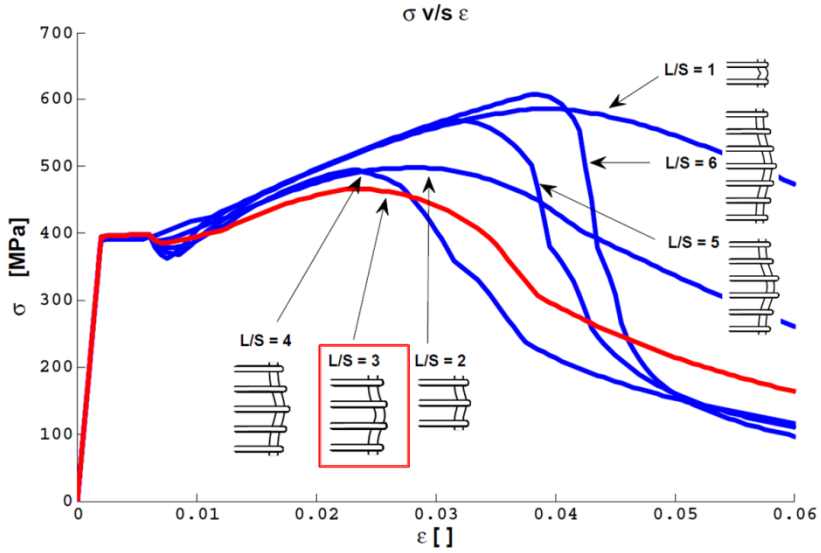

Figure 6. Stress vs. strain response for several buckling modes and criteria selection

4. MODEL RESULTS FOR BUCKLING OF GROUP BARS

Several tests have been carried out to evaluate global and local buckling for columns with concentric axial load (e.g., Kato et al., 1995, Ooya and Kato, 1994, Masamoto et al., 1993, and Kikukawa et al., 1994). The high steel reinforcement (D13H-1) was not considered in the analysis, given the large difference observed for both models (6 cases). The columns had an square section with a core confined dimension estimated as l = 130 mm and a total length of L = 530 mm. The spacing of the stirrups ranged from $1.5d_b$ to $11d_b$, where d_b is the longitudinal rebar diameter, with most test in the range $4d_b$ to $6d_b$. Some columns presented stirrup in intermediate longitudinal bars (for either 8 or 12 total longitudinal reinforcing bars, 4 bar columns were also tested). The rebar yield stress for the specimens considered for comparison ranged from 336 to 761 MPa, whereas the concrete strength ranged from 22 to 70 MPa for a total of 68 tests. The material information is based on σ_y and σ_m, as well as the stress-strain response in tension for most cases, which are available in the literature.

Experimental results are compared to the buckling mode obtained with the proposed model for global buckling (MPG) and the model by Dhakal and Maekawa (2002). The results obtained for the

models are shown in Fig. 7b, and the error between the experimental observation and the buckling modes obtained with the models are shown in Fig. 7(a). The error, in this case, is calculated as $Error_{Mode} = Mode_{Model} - Mode_{Test}$. Fig. 7 shows that the model yields global buckling modes lower than those observed experimentally with slightly higher errors (avg = -0.59, std = 0.88) than those obtained by applying the methodology by Dhakal and Maekawa (2002), which gives an average error of -0.26 and standard deviation of 0.73. As it can be seen in Fig. 7a, most cases show an error of 0 or -1, indicating that the model fails to predict the number of stirrups within the buckled shape commonly in 0 or 1 (less than observed) unit. Fig. 7b shows the correlation between the observed and predicted buckling mode for all cases. Perfect correlation would results in a diagonal representation. The numbers within the circles (and size – the bigger the size, the larger number of cases) correspond to the number of occurrence cases. Although the differences, the model described in this study also allows defining the overall stress vs. strain curve for the buckled bars which can be used in sectional or elements, such as columns or walls, nonlinear analysis.

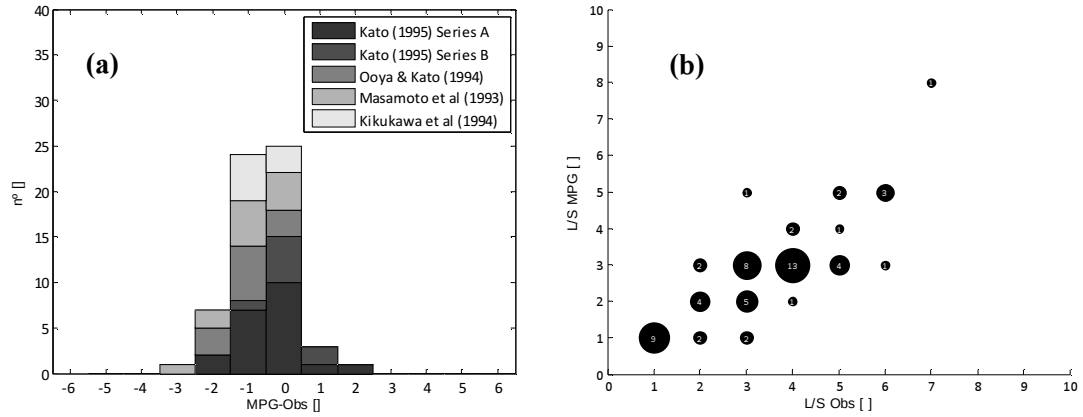

Figure 7. Model results – (a) Error, (b) observed vs. model prediction bucking mode.

5. SUMMARY AND CONCLUSIONS

The objective of this study is to represent the behavior of the longitudinal reinforcement in monotonic compression buckling considering the instability of the bar at a length that exceeds the distance between the stirrups and introducing the effect of transverse reinforcement and concrete core expansion in the analysis. For these purposes the model by Massone and Moroder (2009) for local buckling of reinforcement, based on 4 plastic hinges, is adjusted to introduce the forces associated with transverse reinforcement within the buckling length and the effect of concrete expansion. Forces generated on stirrups beyond the action of the concrete expansion are balanced with the internal moment in the buckled bar.

In terms of the buckling mode obtained with the model, expressing it as the amount of stirrup spacing L/S, the results are relatively good yielding an error comparable to the model by Dhakal and Maekawa (2002), with an average error of -0.59 (about half a stirrup spacing) which is a good value, considering that the used test database has buckling modes ranging from 1 to 7. The methodology used for determining the buckling mode involves generating curves for several possible cases, thus, alternatively, the formulation by Dhakal and Maekawa (2002) could be used to select the buckling mode. The model described in this study, differently than most previous works, besides of predicting the buckling mode, provides the stress-strain curve for the buckled bars (σ-ε) which can be used in sectional or element analysis.

ACKNOWLEDGEMENTS

This work was partially financially supported by Chile's National Commission on Scientific and Technological Research (CONICYT) for the project Fondecyt 2008, Initiation into Research Funding Competition, under Grant No. 11080010.

REFERENCES

Dhakal, R., and Maekawa, K. (2002). Reinforcement stability and fracture of cover concrete in reinforced concrete members. Journal of Structural Engineering ASCE, 128:10, 1253-1262.

Dodd, L.L., Restrepo-Posada, J.I (1995). Model for predicting cyclic behavior of reinforcing steel. Journal of Structural Engineering ASCE, 121:3, 433-45.

Kato, D., Kanaya, J., and Wakatsuki, J. (1995). Buckling strains of main bars in reinforced concrete members. Proc., 5th East Asia and Pacific Conf. in Structural Engineering and Construction EASEC-5, Gold Coast, Australia. , 699-704.

Kikukawa, T., Ooya, H., Kato, D., & Wakatsuki, K. (1994). Buckling behaviors of intermediate steel bars in R/C Columns (in Japanese). Summaries of technical papers of Annual Meeting Architectural Institute of Japan. Structures II , 353-356.

Lacaze, C. (2009). Study and modeling of the impact of buckling in low cycle fatigue in reinforcing bars for reinforced concrete (in Spanish). Civil Engineering Thesis, University of Chile.

Mander, J., Priestley, M., and Park, R. (1988). Theoretical Stress-Strain Model for Confined Concrete. Journal of Structural Engineering ASCE, 114:8, 1804-1826.

Mander, J.B., Priestley, M.J.N., Park R. (1984). Seismic design of bridge piers. Department of civil engineering, University of Canterbury. Report 84-2. 483 pp.

Masamoto, K., Wakatsuki, K., Ooya, H., and Kato, D. (1993). Buckling Behvaviors of Steel Bars in R/C columns (in Japanese). Summaries of technical papers of Annual Meeting Architectural Institute of Japan. Structures II , 787-792.

Massone, L., and Moroder, D. (2009). Buckling modeling of reinforcing bars with imperfections. Engineering Structures, 31:3, 758-767.

Menegotto, M., and Pinto, P.E. (1973). Method of analysis for cyclically loaded reinforced concrete plane frames including changes in geometry and non-elastic behavior of elements under combined normal force and bending. In: Proceedings, IABSE symposium.

Ooya, H., and Kato, D. (1994). Experimental study on buckling behavior of intermediate longitudinal bars in R/C members. Transaction of the Japan Concrete Institute Vol. 16 , 365-372.

Pantazopoulou, S. (1998). Detailing for reinforcement stability in RC members. Journal of Structural Engineering ASCE, 124:6, 623-632.

Papia, M., Russo, G., and Zingone, G. (1988). Instability of longitudinal bars in RC columns. Journal of Structural Engineering ASCE, 114:2, 445-461.

Sheikh, S., and Uzumeri, S. (1980). Analytical model for concrete confinement in tied columns. Journal of the Structural Division, 108:12, 2703-2722.